Laser Mass Spectrometric Analysis of Organic Atmospheric Aerosols. 2. Elucidation of Urban Air Pollution Processes

3 AUTHORS, INCLUDING:

Olivier P Haefliger
Firmenich Aromatics (China) Co., Ltd.
31 PUBLICATIONS **472** CITATIONS

Renato Zenobi
ETH Zurich
459 PUBLICATIONS **13,155** CITATIONS

Laser Mass Spectrometric Analysis of Organic Atmospheric Aerosols. 2. Elucidation of Urban Air Pollution Processes

OLIVIER P. HAEFLIGER,
THOMAS D. BUCHELI, AND
RENATO ZENOBI*

Department of Chemistry, Swiss Federal Institute of Technology (ETH), Universitätstrasse 16, CH-8092 Zurich, Switzerland

The dynamic behavior of aerosol-bound polycyclic aromatic hydrocarbons (PAHs) and other polycyclic aromatic compounds (PACs) in urban air was studied over the course of several whole days, both next to a street with heavy traffic and in a city park. Two-step laser mass spectrometry, a highly sensitive and selective technique, allowed measurements with 15 min time resolution. Large variations in particle concentration and chemical composition were observed, reflecting the contributions from Diesel trucks and gasoline-powered cars to urban aerosols. These sources were clearly identified using specific mass spectral patterns. Photochemically induced decay of oxygenated polycyclic aromatic hydrocarbons (OPAHs) was observed to occur within only a few hours. Rapid speciation of aerosol-bound organic carbon is now possible to complement data on routinely monitored atmospheric pollutants.

Introduction

Carbonaceous aerosol particles given off during the combustion of organic material are known to play a key role in environmental processes (*1, 2*) and to be hazardous for human health (*3*). Their physical properties and their chemical composition however can strongly vary depending on their emission source. These can include Diesel vehicles, gasoline vehicles, residential heating, wood fires, or cigarettes (*4–8*). The relative contributions of different emission sources to the total aerosol load at urban sites of exposure change on a short time-scale and are dependent for example on traffic rush hours, residential heating cycles, and meteorological parameters such as wind intensity, precipitation, and solar irradiation. A true understanding of the processes that aerosols take part in therefore requires characterization measurements to be performed on a time scale similar to these dynamic changes. The techniques commonly used to determine the chemical composition of particles are chromatographic methods for the quantitation of organic compounds and ions (*4, 9–16*) and atomic spectroscopic methods for the determination of the elemental composition (*16–18*). They usually require tedious and time-consuming sample preparation as well as the collection of relatively large sample quantities on filters over extended periods of time, generally 24 h, even in polluted urban areas. They are

* Corresponding author phone: +41-1-632 4376; fax: +41-1-632 1292; e-mail: zenobi@org.chem.ethz.ch.

therefore not well-suited for the real-time identification of emission sources. Studies with a time resolution on the scale of 1 or 2 h remain exceptions (*14, 19, 20*).

A technique specifically developed for particle measurements with high time resolution is single particle laser desorption/ionization mass spectrometry (LDI-MS) (*21–23*). Single particle LDI-MS allows online sizing and chemical analysis of single aerosol particles and the identification of their emission sources according to their inorganic composition (*24, 25*). However, any classification based on the organic composition of the particulates, for example for the identification of different combustion emission sources, is still problematic because characteristic organic tracer analytes (*4–7*) fragment extensively during LDI-MS analysis. Also, direct comparison with data obtained using conventional methods for monitoring gaseous or particle-bound atmospheric pollutants is not possible due to poorly characterized particle-size dependent sampling efficiency and particle-type dependent ion generation.

In an effort to identify the relevant urban aerosol emission sources, we have adapted two-step laser mass spectrometry (L2MS) (*26–30*) to follow the evolution of selected tracer molecules. L2MS uses samples collected on filters and therefore allows quantitative analyses of particle-bound organic compounds (*31*). In addition, data can be obtained within minutes through direct measurements, with a sensitivity in the low attomole range for some analyte compounds. L2MS therefore permits the analysis of a large number of samples, collected during short periods of time.

In a companion paper, we have shown how L2MS allows the identification of various aerosol emission sources based on tracer mass spectral patterns, notably specific polycyclic aromatic compounds (PACs) (*32*). This paper now reports on field studies at urban sites of exposure during which these tracers were monitored with a 15 min time resolution over the course of several whole days. First, principal component analysis (PCA) was performed on the data, which confirmed the reliability of the identified tracers. The different developments of the relative amounts of the tracer compounds then allowed the evaluation of the importance of the contributions of different emission sources as a function of time.

Experimental Section

Sampling Technique. The custom designed filter holders described previously (*32*) were used for both sampling and L2MS measurements without further manipulation. Standard quarz fiber filters (Pallflex, Putnam, CT) were used for sampling, and no information on the size distribution of the particles was therefore available. The samples were stored under argon, at 2 °C, in the dark, and were measured within less than 20 h.

Study of the Variation during the Day. Measurement campaigns were conducted in the summer (June and July 1998, two weekdays and two Sundays) as well as in the winter (January and February 1999, two weekdays and two Sundays) in Zurich, Switzerland. The buildings are not heated in summer so that this emission source is only relevant during the winter. Sampling was performed with 15 min time resolution at daytime (from about 4:30 to 21:30) and 30 min time resolution at night time. The first sampling site was located in the city center next to a street with heavy urban and transit traffic (about 30 000 vehicles a day) and is therefore typical for street emissions. Comparative urban background measurements were simultaneously performed in a city park enclosed by buildings. The distance between the two sites is about 900 m. Both sites are part of the official Swiss
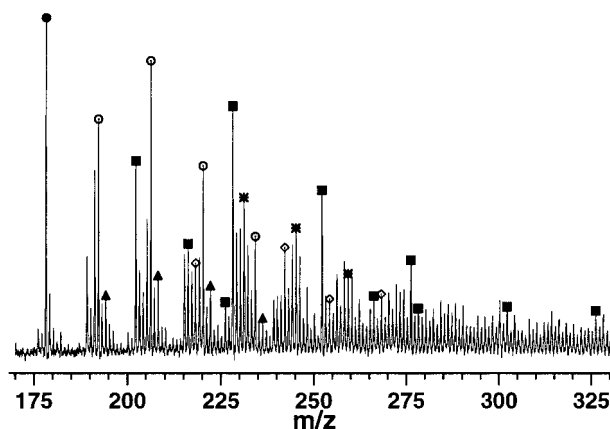
FIGURE 1. Example of a L2MS spectrum. Street site, Wednesday, July 1998, sampling between 5:45 and 5:59. Average of 49 shots on different spots of the filter sample. The peaks used for PCA are marked. ●: Phenanthrene (178). ○: C_n-alkylphenanthrenes (192, 206, 220, 234). ■: PAHs (202, 216, 226, 228, 252, 266, 276, 278, 302, 326). ∗: m/z = 231 family (231, 245, 259). ▲: Oxygenated PAHs (194, 208, 222, 236). ◇: Other peaks (218, 242, 254, 268).

monitoring network (Nationales Beobachtungsnetz für Luftfremdstoffe, NABEL) so that records of all main standard gaseous pollutants, of black carbon (BC), and of weather data were available for comparison. Furthermore, trucks and cars passing at the street site were counted.

L2MS System. The L2MS measurements were performed on the same instrument used for the characterization of the emission sources mentioned previously, run under identical conditions (*32*). The peak intensities were averaged over about 50 single shots on different spots for each sample. Their standard deviations were around 10–20%.

Principal Component Analysis. Principal component analysis (PCA) is a technique to reduce the dimensionality of a data set. PCA aims to determine few principal components (PC) that can explain as much of the total variance in the measured data as possible. The PCs are linear combinations of the observed variables, mass spectral peak intensities in the case of this study. After matrix calculations, a *loading* is determined that quantifies the correlation between each pair of observed variable and new PC. A detailed description of the mathematical principles of PCA is beyond the scope of this paper and can be found in the literature (*33–35*). PCA was performed using the data processing software SPLUS (MathSoft, Inc.). After keeping only those PCs with an eigenvalue greater than 70% of the mean of all eigenvalues, orthogonal (varimax) rotation of the loading matrix was performed in order to simplify the interpretation of the results.

Results and Discussion

Principal Component Analysis. Figure 1 shows as an example one of the 1070 averaged L2MS spectra recorded during the measurement campaigns. The peaks previously identified as emission source specific tracers, together with the ones that were found with high signal intensities in the emission profiles, were selected for PCA (*32*). The peaks at several of the PAH skeleton masses and a few whose intensities were remarkably high in the spectrum displayed in Figure 1 or in other mass spectra were included in this data set as well, resulting in a selection of 26 peaks.

Performing PCA on all 1070 mass spectra recorded during the summer and the winter field campaigns, at both sampling sites, led to the identification of four PCs. The results are displayed in Figure 2. A large data set was selected to allow a clearer interpretation. This was possible because the same classes of particles are found at both sampling sites with only their relative proportions varying, and because there

were no major differences between the results of the summer and winter field campaigns. Similar PCs were observed using reduced data sets, for example by analyzing the winter and the summer data separately or by considering only one sampling site at a time.

PC1. PC1 is dominated by phenanthrene and especially by the alkylphenanthrenes. PC1 is in very good agreement with the Diesel truck emission profile of the companion paper (*32*). It therefore most likely reflects the contribution of this emission source.

PC2. PC2 correlates mostly with PAH skeletons. However, none of the studied emission sources, including vehicles, residential heating, wood fires, and cigarettes, was observed to be dominated by PAH skeletons exclusively. Rather than being directly linked to a well-defined emission source, this PC could possibly be assigned to road dust. Road dust is a very complex variable because practically any anthropogenic or biogenic source can add to the dust accumulation on the road surfaces. Contributors include among others particulate vehicle exhaust, lubricating oil residues, tire wear particles, weathered street surface particles, and brake lining particles (*15*). High PAH levels in road dust were reported by Rogge et al. (*15*). Furthermore, Harrison et al. (*36*) have shown that the largest fraction of most PAHs actually stems from road dust and not directly from vehicle exhaust.

PC3. Only the peaks of the m/z = 231 family (*231, 245, 259*) exhibit a strong correlation with PC3. These are the ones that were previously identified as highly specific tracers for gasoline-powered cars so that this PC can be assigned to them (*32*). The distinction between trucks and cars is quite clear-cut in Switzerland because virtually all cars are powered by gasoline engines equipped with catalytic converters. Trucks are therefore by far the main contributors to Diesel exhaust.

PC4. The last of the four PCs, PC4, is the least substance class specific. It is nevertheless dominated by oxygenated polycyclic aromatic hydrocarbons (OPAHs) such as polycyclic aromatic ketones (PAKs) or polycyclic aromatic quinones (PAQs). PC4 could possibly be assigned to open wood fires or properly functioning oil heating systems where these compounds were found at high levels. However, this interpretation does not seem satisfactory since a high correlation with alkylphenanthrenes should also be observed, which is not the case. Rather, PC4 seems to be representative of meteorological parameters, especially the solar irradiance, to which the levels of the OPAHs seem to be especially sensitive. This will be discussed in more detail below.

Summary. Two studies based on completely independent strategies, the direct measurement of emission samples on one hand (*32*) and PCA analysis of samples collected at sites of exposure on the other hand, have shown excellent agreement and resulted in the identification of the same tracer mass spectral patterns. This confirms the suitability of L2MS for the on-site and time-resolved identification of the contributing aerosol emission sources.

Comparison of L2MS vs Black Carbon. Figure 3A shows the variation of a parameter we define here as S26, the sum of the 26 ion signals selected for PCA (Figure 1), for July 15 (Wednesday) at the street site. The dynamic behavior is striking, with a sharp increase starting around 5:00. The lowest values were observed at night when the traffic intensity was low. For comparison, Figure 3B displays the black carbon (BC) concentration monitored simultaneously by an aethalometer (AE-10, Magee Scientific Co., Berkeley, CA). Both temporal developments look quite similar. Even spikes can be observed in both curves at the same times, for example around 7:30, 9:45, or 15:00. Hence, S26 is found to correlate with the total amount of carbonaceous particles present. This result demonstrates the ability of L2MS to provide accurate data that can be directly and quantitatively com-
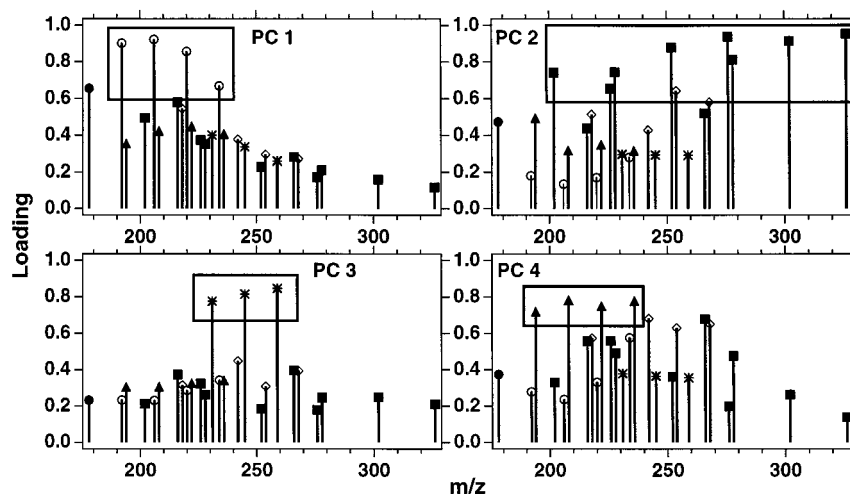
FIGURE 2. Results of the PCA on all of the 1070 mass spectra recorded during the summer and winter field campaigns, at the two sampling sites. ●: Phenanthrene (178). ○: C_n-alkylphenanthrenes (192, 206, 220, 234). ■: PAHs (202, 216, 226, 228, 252, 266, 276, 278, 302, 326). ∗: m/z = 231 family (231, 245, 259). ▲: Oxygenated PAHs (194, 208, 222, 236). ◇: Other peaks (218, 242, 254, 268). See text for the assignment of the PCs.
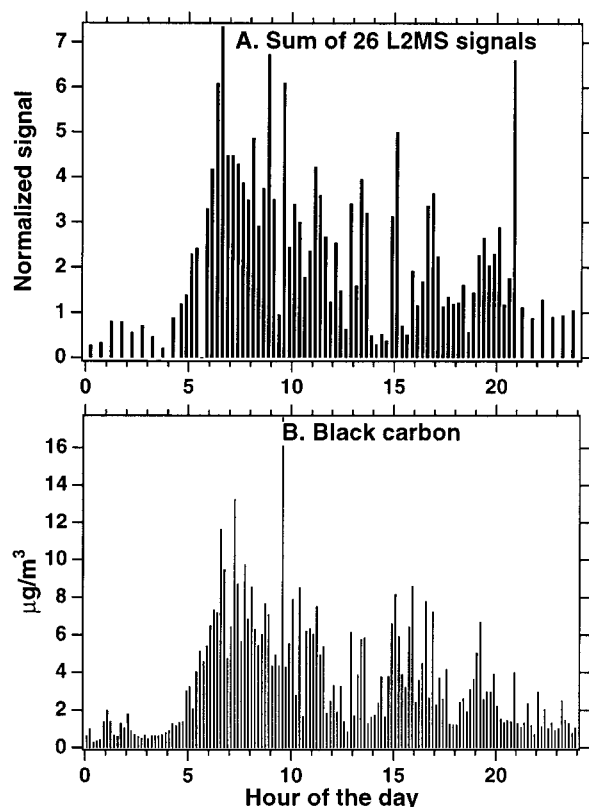

FIGURE 3. Temporal developments recorded at the street site on Wednesday, July 15, 1998. (A) S26, the sum of the ion signals at the 26 selected peaks (see text), monitored by L2MS (15 min. intervals). (B) Black carbon, monitored by an aethalometer (10 min intervals).

pared to data obtained using standard monitoring techniques. A rather fast spreading of the combustion aerosols within the area under investigation can be implied based on the observation that no lag was observed between the rush hours and the increase of the pollutant signals at the park site (data not shown).

The peak around 20:45 in Figure 3, which is present in the BC curve and especially intense in the S26 curve, deserves further discussion. This data point is not an experimental artifact. The high intensity is only due to certain mass spectral peaks. All of them correspond to dominant peaks in the
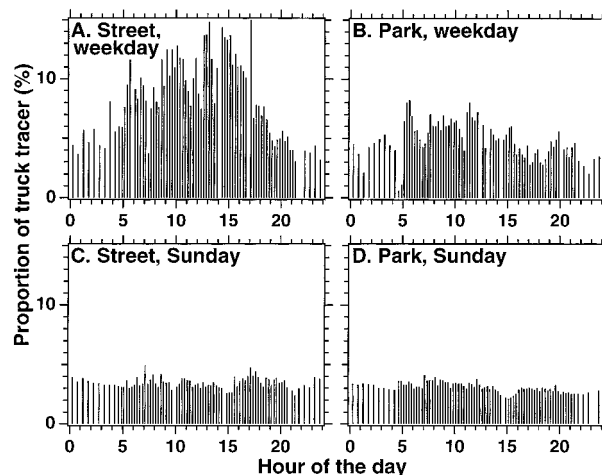

FIGURE 4. Variation of the proportion of a truck tracer (ion signal at m/z = 206) over the course of entire days. (A) Street site, Wednesday, February 10, 1999. (B) Park site, Wednesday, February 10, 1999. (C) Street site, Sunday, January 24, 1999. (D) Park site, Sunday, January 24, 1999.

previously reported emission profile of Diesel engine exhaust (32). Therefore, the high levels observed for these analytes at 20:45 were probably caused by one or several vehicles with poorly running Diesel engines that passed by the sampling site at that particular time. This type of observation clearly proves that L2MS can provide much more detailed information than BC. Indeed, the parameter S26, although being useful to provide information on the concentration of carbonaceous particles, loses the emission source specificity of its separate components. It is much more interesting to consider the temporal development of single masses, as will be shown now.

Temporal Development of Trucks and Car Tracers. Similar behaviors of these tracers were observed in winter and in summer, although the total particle concentration was higher in winter. This confirms what we observed during the characterization of the emission sources (32), namely that the low particulate emission generated by residential heating makes this source unlikely to be an important one in Zurich.

Figures 4 and 5 display the temporal evolution of the proportion of tracer peaks for trucks (Figure 4) and cars (Figure 5) at both sites, on a weekday (Wednesday, February
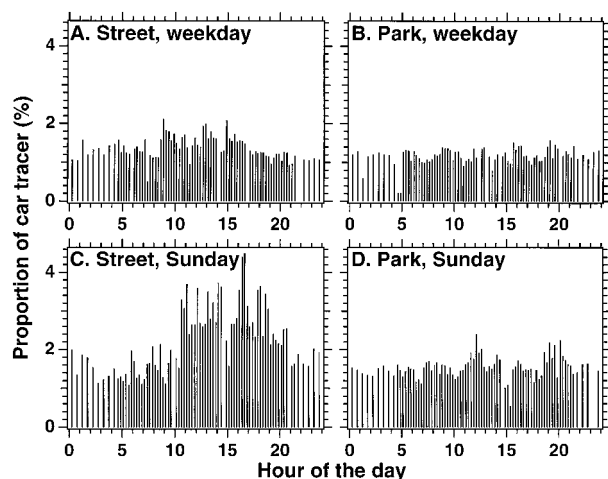
FIGURE 5. Variation of the proportion of a car tracer (ion signal at $m/z = 231$) over the course of entire days. (A) Street site, Wednesday, February 10, 1999. (B) Park site, Wednesday, February 10, 1999. (C) Street site, Sunday, January 24, 1999. (D) Park site, Sunday, January 24, 1999.
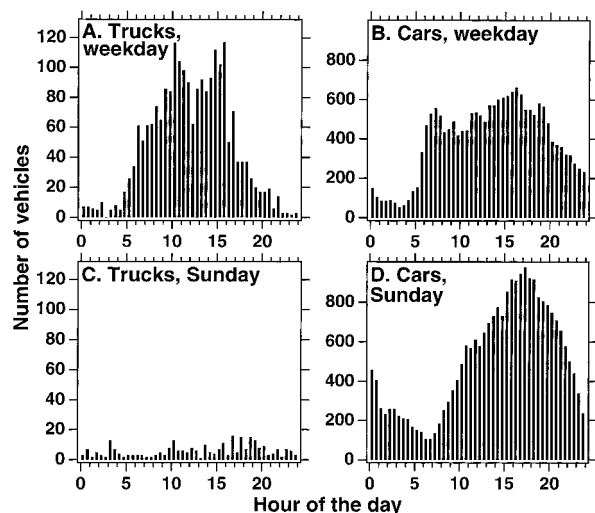

FIGURE 6. Traffic numbers at the street site. (A) Trucks, Wednesday, February 10, 1999. (B) Cars, Wednesday, February 10, 1999. (C) Trucks, Sunday, February 14, 1999. (D) Cars, Sunday, February 14, 1999.

10, 1999) and on a Sunday (January 24, 1999). The ion signal at $m/z = 206$, which corresponds to C_2-alkylphenanthrenes, was selected to represent trucks because it was the dominant one in the Diesel exhaust emission profile (*32*) and also the one with the highest correlation with the principal component related to trucks (Figure 2). The ion signal at $m/z = 231$, which may correspond to methylbenzocarbazoles (*32*), was selected to represent cars because it was the most intense one in the car emission profiles, and therefore the one most likely to be detected at remote sites where the concentration of car aerosol may be low. The displayed proportions were calculated by dividing the ion signals at $m/z = 206$ and 231 by the summed ion signal from S26. The S26 factor correlates with the concentration of carbonaceous particles in air (see above). This normalization was necessary to provide a clearer comparison between the behavior of different analytes at different sites on different days.

To better understand the behavior of the tracer peaks, Figure 6 displays the traffic numbers recorded for trucks and cars at the street site on a weekday (Wednesday, February 10, 1999) and on a Sunday (February 14, 1999). The traffic patterns observed for trucks are due to the strict air quality and traffic regulations in Switzerland. Truck traffic is banned

on Sundays as well as on working days between 22:00 and 06:00. Virtually no variation in traffic patterns was observed between different weekdays and between different Sundays (data not shown) so that the data plotted in Figure 6 (parts C and D) can reasonably be used to discuss the L2MS data recorded on Sunday, January 24 for which no traffic numbers were available.

Let us first compare the street emissions on the weekday to the ones on the Sunday. The concentration of the truck tracer remained at low levels during the whole Sunday (Figure 4C) as well as during the night on Wednesday (Figure 4A), for those periods when truck traffic is forbidden. In contrast, a significant increase was observed during the day on Wednesday. Similar patterns were also observed for the other alkylphenanthrenes observed in the Diesel emission profile ($m/z = 192, 220, ...$) and for the other sampling days in winter and in summer. The behavior of the car tracer was complementary: while an almost constant level was observed on Wednesday (Figure 5A), a strong increase was observed on Sunday between 10:00 and 20:00, that is when car traffic was most intense (Figure 5C). It should be noted that increases in the proportion of the respective tracers occurring to a similar extent, that is roughly to a doubling of the proportion, were in one case caused by about 200 trucks per hour and in the other case by about 1600 cars per hour. This confirms that particulate emissions are much stronger from trucks than from cars. It also explains why the daytime increase in the proportion of the car tracer (Figure 5A) is partly suppressed by the concomitant increase of S26 caused by the truck tracer peaks.

The discussion can now be extended to the data for the urban background at the park site recorded in parallel to the street emission measurements. Figure 4B shows that the daytime proportion of dimethylphenanthrenes is also enhanced at the park site, although to a lesser extent than at the street site. This evidences the transport and dilution by mixing of the particles between both sampling sites. The fact that Diesel exhaust particles are not as dominant at the park site as at the street site may be due to the fact that an important fraction of the aerosol particles that reach the park site originate from other emission sources, in particular from streets in the vicinity which mainly carry local car traffic, and not only from a few transit streets with a large number of trucks. Hence, data collected close to a strong emission source cannot be considered to be representative of urban background sites, not even nearby ones. Official air pollution monitoring sites should therefore be selected not only near emission sources but also at locations where the population is more typically exposed to air pollution. A similar conclusion can be reached from Figure 5D: the high level of the car tracer observed during daytime at the street site is hardly observed at all at the park site.

Direct Observation of Atmospheric Photochemical Processes. Figure 7A displays the temporal variation of the proportion of the OPAHs at $m/z = 208$ on Sunday, January 24, 1999 at the park site. All other suggested OPAHs ($m/z = 194$: anthrone, phenanthrone; $m/z = 208$: anthraquinone, phenanthrenequinone; $m/z = 222$: C_1-alkyl-208; $m/z = 236$: C_2-alkyl-208) exhibited the same behavior. Table 1 summarizes the behaviors observed for all 26 components of S26 during the event. The dramatic decrease of the proportion of the OPAHs between 10:30 and 20:00 took place in parallel with a major increase of pyrene and especially phenanthrene as shown by Figure 7B. The behavior of the OPAHs on that day was especially remarkable because it was the only case during our measurement campaigns where major changes in the levels of certain analytes occurred to the same extent at both the park site (Figure 7A) and the street site (data not shown). This is a clear indication that the observed variations were not simply caused by changes in the relative intensity
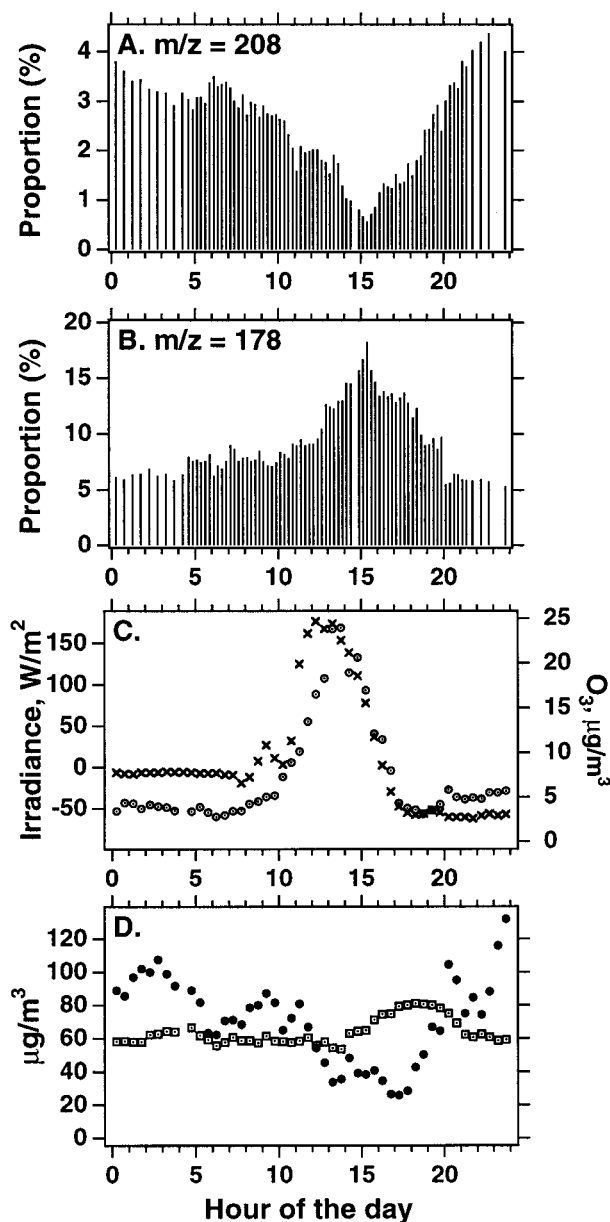
FIGURE 7. Temporal developments at the park site, Sunday, January 24, 1999. (A) Proportion of a typical oxygenated PAH (ion signal at m/z = 208). (B) Proportion of the ion signal at m/z = 178 (phenanthrene). (C) ×: Balanced irradiance. ○: O_3. (D) ●: NO. □: NO_2. The data were recorded simultaneously and at the same location as for the Figures 4D (truck tracer) and 5D (car tracer).

TABLE 1. Variation of the Proportion of the Components of S26 on January 24, 1999 between 10:30 and 20:00 at the Park Site

behavior	analytes
major decrease	m/z = 194, 208, 222, 236 OPAHs C_4-alkylphenanthrenes
medium decrease	m/z = 242, 268 compounds
minor decrease	m/z = 218, 254 compounds C_2- and C_3-alkylphenanthrenes m/z = 266, 278 PAHs
constant	m/z = 231, 245, 259 car tracers m/z = 226, 228, 252, 276, 302, 326 PAHs
minor increase	m/z = 216 PAHs C_1−alkylphenanthrenes
major increase	m/z = 178 (phenanthrene) m/z = 202 (pyrene)

Furthermore, such a strong contribution from an emission source would have induced an increase of the BC concentration and of the overall intensity of S26, which were not observed (data not shown).

It is therefore more than likely that degradation of the OPAHs was due to atmospheric chemical reactions induced by intense solar irradiance. The especially high balanced irradiance in the afternoon of January 24, 1999 (Figure 7C) initiated photochemical ozone formation from NO_2 and O_2 between 10:00 and 16:30. This reaction and the simultaneous ozone degradation through its reaction with NO to regenerate NO_2, form a cycle (37, 38). This mechanism, together with the partial disappearance of the inversion layer during the day and the corresponding enhanced dilution, explains the variation of the concentrations of O_3 (Figure 7C), NO (Figure 7D), and NO_2 (Figure 7D) during the afternoon. The NO concentration started to rise again after the disappearance of the sun at 16:30 and reached its initial level around 20:00. The close similarity between the evolution of the NO concentration and that of the OPAH proportion, with virtually simultaneous start and finish of the event, seems to indicate that these compounds may undergo similar degradation reactions, such as oxidation by O_3 or by OH-radicals. The detailed reaction pathways leading to degradation of the OPAHs however remain unknown. A better understanding of these processes would in also contribute elements to explain the increases in proportion of phenanthrene and pyrene which seem to be intimately linked with them.

Overview and Outlook

Our results clearly demonstrate that by monitoring the sum parameter S26, L2MS provides quantitative information similar to the BC concentration (Figure 3). In addition, the possibility to follow the variation of tracers at specific masses makes the identification of emission sources possible. The use of tracers for this purpose has already been described in detail by several researchers (4, 14, 20). This report, however, introduces a new analytical tool that can accomplish the same task with much higher time resolution. The agreement between the new L2MS data shown here and the results simultaneously obtained for other major pollutants and traffic intensity confirms the suitability of L2MS for real-world studies. Further developments of the method for routine operation could include the design of a small, portable field instrument, the use of alternative ionization laser wavelengths adapted to organic compounds other than PAHs, and an interface that would allow automated on-site measurements immediately after aerosol sampling.

The results presented here are not only useful for studying aerosol emission sources. The fact that the relative contributions of the ion signals at the different masses do not remain constant implies that the molecular composition of the

of the particulate emission of urban vehicular sources. In this case the changes would have been more pronounced at the street site than at the park site. Note that for this specific reason, the increase of the proportion of phenanthrene was less pronounced at the street site (data not shown) than at the park site (Figure 7B).

A possible explanation for the behaviors observed in Figure 7 (parts A and B) could be that the total aerosol load as quantified by S26 at that particular time was dominated and significantly increased by the contribution from an unusually intense remote or ubiquitous emission source such as an explosion. This hypothesis can however be ruled out because a strong increase was only observed for phenanthrene and pyrene among all the components of S26. No emission source was identified neither by us (32) nor, to the best of our knowledge, by other authors that gives off particles loaded with high amounts of these two compounds exclusively.

organic carbon fraction of urban aerosol particles is highly variable in time. The possibility to use L2MS to measure these dynamic changes in the molecular composition of aerosol particle surfaces with high time resolution opens new avenues for studying emission and transport dynamics, heterogeneous chemistry, and health hazards linked to aerosol particles.

Acknowledgments

Literature Cited

(1) Pandis, S. N.; Wexler, A. S.; Seinfeld, J. H. *J. Phys. Chem.* **1995**, *99*, 9646−9659.

(2) Finlayson-Pitts, B. J.; Pitts, J. N. *Science* **1997**, *276*, 1045.

(3) Schlesinger, R. B. *Inh. Tox.* **1995**, *7*, 99−109.

(4) Rogge, W. F.; Hildemann, L. M.; Mazurek, M. A.; Cass, G. R.; Simoneit, B. R. T. *Environ. Sci. Technol.* **1993**, *27*, 636−651.

(5) Rogge, W. F.; Hildemann, L. M.; Mazurek, M. A.; Cass, G. R.; Simoneit, B. R. T. *Environ. Sci. Technol.* **1994**, *28*, 1375−1388.

(6) Rogge, W. F.; Hildemann, L. M.; Mazurek, M. A.; Cass, G. R.; Simoneit, B. R. T. *Environ. Sci. Technol.* **1997**, *31*, 2731−2737.

(7) Rogge, W. F.; Hildemann, L. M.; Mazurek, M. A.; Cass, G. R.; Simoneit, B. R. *Environ. Sci. Technol.* **1998**, *32*, 13−22.

(8) Miguel, A. H.; Kirchstetter, T. W.; Harley, R. A. *Environ. Sci. Technol.* **1998**, *32*, 450−455.

(9) Lee, M. L.; Novotny, M. V.; Bartle, K. D. *Analytical Chemistry of Polycyclic Aromatic Compounds*; Academic Press: New York, 1981.

(10) Gao, N.; Cheng, M. D.; Hopke, P. K. *Atmos. Environ.* **1994**, *28*, 1447−1470.

(11) Peltonen, K.; Kuljukka, T. *J. Chromatogr. A* **1995**, *710*, 93−108.

(12) Rahmalan, A.; Abdullah, M. Z.; Sanagi, M. M.; Rashid, M. *J. Chromatogr. A* **1996**, *739*, 233−239.

(13) Fraser, M. P.; Cass, G. R.; Simoneit, B. R. T. *Environ. Sci. Technol.* **1998**, *32*, 2051−2060.

(14) Nielsen, T. *Atmos. Environ.* **1996**, *30*, 3481−3490.

(15) Rogge, W. F.; Hildemann, L. M.; Mazurek, M. A.; Cass, G. R.; Simoneit, B. R. T. *Environ. Sci. Technol.* **1993**, *27*, 1892−1904.

(16) Mateu, J.; Forteza, R.; Cerda, V.; Colomaltes, M. *Water, Air, Soil Pollut.* **1995**, *84*, 61−79.

(17) Wang, C. F.; Chang, E. E.; Chiang, P. C.; Aras, N. K. *Analyst* **1995**, *120*, 2521−2527.

(18) Jalkanen, L. M.; Hasanen, E. K. *J. Anal. Atom. Spectrom.* **1996**, *11*, 365−369.

(19) Koeber, R.; Bayona, J. M.; Niessner, R. *Environ. Sci. Technol.* **1999**, *33*, 1552−1558.

(20) Lim, L. H.; Harrison, R. M.; Harrad, S. *Environ. Sci. Technol.* **1999**, *in press*.

(21) Johnston, M. V.; Wexler, A. S. *Anal. Chem.* **1995**, *67*, 721−726.

(22) Gard, E.; Mayer, J. E.; Morrical, B. D.; Dienes, T.; Fergenson, D. P.; Prather, K. A. *Anal. Chem.* **1997**, *69*, 4083−4091.

(23) Gard, E. E.; Kleeman, M. J.; Gross, D. S.; Hughes, L. S.; Allen, J. O.; Morrical, B. D.; Fergenson, D. P.; Dienes, T.; Gälli, M. E.; Johnson, R. J.; Cass, G. R.; Prather, K. A. *Science* **1998**, *279*, 1184−1187.

(24) Hinz, K. P.; Kaufmann, R.; Spengler, B. *Aerosol Sci. Technol.* **1996**, *24*, 233−242.

(25) Murphy, D. M.; Thomson, D. S.; Mahoney, M. J. *Science* **1998**, *282*, 1664−1669.

(26) Voumard, P.; Zhan, Q.; Zenobi, R. *Rev. Sci. Instrum.* **1993**, *25*, 3393−3402.

(27) Haefliger, O. P.; Zenobi, R. *Anal. Chem.* **1998**, *70*, 2660−2665.

(28) Clemett, S. J.; Maechling, C. R.; Zare, R. N.; Swan, P. D.; Walker, R. M. *Science* **1993**, *262*, 721−724.

(29) Dale, M. J.; Jones, A. C.; Pollard, S. J. T.; Langridge-Smith, P. R. R. *Analyst* **1994**, *119*, 517−578.

(30) Zhan, Q.; Voumard, P.; Zenobi, R. *Rapid Commun. Mass Spectrom.* **1995**, *9*, 119−127.

(31) Haefliger, O. P.; Zenobi, R. *Rev. Sci. Instrum.* **1998**, *69*, 1828−1832.

(32) Haefliger, O. P.; Bucheli, T. D.; Zenobi, R. *Environ. Sci. Technol.* **2000**, *34*, 2178−2183.

(33) Pearson, K. *On the theory of contigency and its relation to association and normal correlation*; University Press: Cambridge, 1904.

(34) Hotelling, H. *J. Educ. Psych.* **1933**, *24*, 417−441, 498−520.

(35) Sirois, A. *PCA and other dimensionality reduction techniques: a short overview;* at the Workshop on advanced statistical methods and their application to air quality data sets; Helsinki, 1998.

(36) Harrison, R. M.; Smith, D. J. T.; Luhana, L. *Environ. Sci. Technol.* **1996**, *30*, 825−832.

(37) Seinfeld, J. H. *Air Pollution*; John Wiley and Sons: New York, 1986.

(38) Finlayson-Pitts, B. J.; Pitts, J. N. *Atmospheric Chemistry*; John Wiley and Sons: New York, 1986.